The Reduced, Denatured Somatomedin B Domain of Vitronectin Refolds into a Stable, Biologically Active Molecule†

Yuichi Kamikubo,‡ Gerard Kroon,§ Scott A. Curriden,‡ H. Jane Dyson,*,§ and David J. Loskutoff‡

Department of Cell Biology, Division of Vascular Biology, and Department of Molecular Biology and Skaggs Institute for Chemical Biology, The Scripps Research Institute, 10550 North Torrey Pines Road, La Jolla, California 92037

Received November 7, 2005; Revised Manuscript Received January 17, 2006

ABSTRACT: The high-affinity binding site in human vitronectin (VN) for plasminogen activator inhibitor-1 (PAI-1) has been localized to the NH_2-terminal cysteine-rich somatomedin B (SMB) domain (residues 1−44). A number of published structural and biochemical studies show conflicting results for the disulfide bonding pattern and the overall fold of the SMB domain, possibly because this domain may undergo disulfide shuffling and/or conformational changes during handling. Here we show that bacterially expressed recombinant SMB (rSMB) can be refolded to a single form that shows maximal activity in binding to PAI-1 and to a conformation-dependent monoclonal antibody (mAb 153). The oxidative refolding pathway of rSMB can be followed in the presence of glutathione redox buffers. This approach allowed the isolation and analysis of a number of intermediate folding species and of the final stably folded species at equilibrium. Competitive surface plasmon resonance analysis demonstrated that the stably refolded rSMB regained biological activity since it bound efficiently to PAI-1 and to mAb 153. In contrast, none of the folding intermediates bound to PAI-1 or to mAb 153. We also show by NMR analysis that the stably refolded rSMB is identical to the material used for the solution structure determination [Kamikubo et al. (2004) *Biochemistry 43*, 6519] and that it binds specifically to mAb 153 via an interface that includes the three aromatic side chains previously implicated in binding to PAI-1.

Vitronectin (VN) is a 75 kDa adhesive glycoprotein found in the circulation and extracellular matrix of many tissues (*1*). It plays a significant role in a number of physiological processes such as cell adhesion, cell migration, modulation of the immune system, and regulation of blood coagulation and fibrinolysis (*1*, *2*). This range of functions seems to reflect the ability of VN to interact with numerous partner proteins (*3*). One important binding partner for VN is type 1 plasminogen activator inhibitor (PAI-1), the primary inhibitor of both tissue- and urokinase-type plasminogen activators. Although PAI-1 is a member of the serine protease inhibitor (serpin) superfamily, it has several unique properties that distinguish it from other serpins (*4*). For example, PAI-1 is conformationally unstable (*5*), and it rapidly decays into an inactive "latent" form in solution by spontaneous insertion of its reactive center loop (RCL) into the main β-sheet of the molecule (*6*−*8*). Moreover, PAI-1 is a trace protein in blood, and it circulates in complex with VN (*9*−*12*). PAI-1 binds to VN with high affinity, and this interaction stabilizes the inhibitor in its active conformation by restricting movement of the RCL of the inhibitor and preventing its insertion (*13*, *14*). The binding of PAI-1 to VN also alters the adhesive properties of VN, and it is now clear that PAI-1 regulates cell adhesion and migration on VN (*15*−*18*). The interaction between PAI-1 and VN may also be clinically important since elevated levels of active PAI-1 are not only associated with several thrombotic diseases such as myocardial infarction and deep vein thrombosis (*19*) but also indicate a poor prognosis for survival in several metastatic human cancers (*20*). These observations suggest that the diverse physiological functions of VN may be mediated, at least in part, through these effects on PAI-1 (*4*, *21*).

The high-affinity binding site for PAI-1 has been localized to the somatomedin B (SMB) domain at the N-terminus (amino acid residues 1−44) of VN (*22*−*24*). The SMB domain contains eight Cys residues arranged into four disulfide bonds, and correct disulfide linkages in this domain are required for PAI-1 binding (*25*−*27*). Several recent studies provide insights into the structure of this important domain. For example, we recently isolated an active form of recombinant SMB (rSMB) from transformed *Escherichia coli* and presented data to suggest that the four disulfide bonds were arranged consecutively in a linear uncrossed pattern (Cys^5−Cys^9, Cys^{19}−Cys^{21}, Cys^{25}−Cys^{31}, and Cys^{32}−Cys^{39}) (see Figure 1A) (*25*). The solution structure of this active form of rSMB was determined by NMR spectroscopy (*28*) and suggested that the four disulfide bonds were tightly packed in the center of the domain, replacing the traditional hydrophobic core expected for a globular protein (Figure 1B). The few non-cysteine hydrophobic side chains (e.g., Leu^{24}, Tyr^{27}, and Tyr^{28}) form a cluster on the outside of the domain, providing a distinctive binding surface for PAI-1 (Figure 1B). This hydrophobic surface consists mainly of side chains from

† This work was supported by NIH Grants HL31950 to D.J.L. and CA27489 to H.J.D.

* Correspondence should be addressed to this author: phone, 858 784 2223; fax, 858 784 9822; e-mail, dyson@scripps.edu.

‡ Department of Cell Biology, Division of Vascular Biology, The Scripps Research Institute.

§ Department of Molecular Biology and Skaggs Institute for Chemical Biology, The Scripps Research Institute.

10.1021/bi052278f CCC: $33.50
Published on Web 02/16/2006

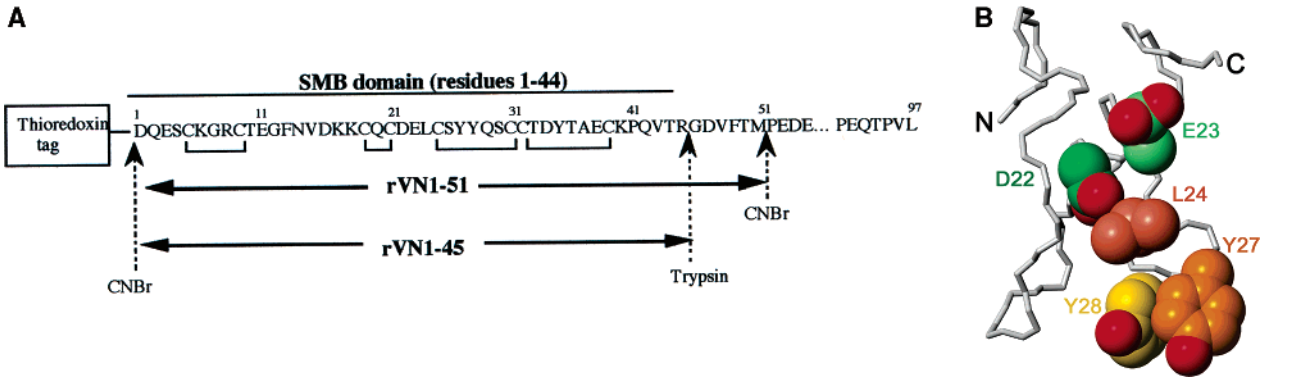

FIGURE 1: Preparation and analysis of the SMB domain. (A) Construct used to express the SMB domain. As indicated, recombinant VN1−51 containing the SMB domain was produced by cyanogen bromide (CNBr) cleavage of rVN1−97 as described (*25*). Recombinant VN1−45 was then prepared by trypsin digestion of rVN1−51. (B) Solution structure of the active form of rSMB (*28*) showing the side chains of residues that have been identified in mutagenesis experiments (*27*) to form the PAI-1 binding site. Side chains of Asp 22 (green), Glu 23 (light green), Leu 24 (coral), Tyr 27 (orange), and Tyr 28 (yellow) are shown in space-filling representation, with oxygen atoms in red. Structure prepared in MOLMOL (*49*).

the loop formed by the Cys^{25}−Cys^{31} disulfide bond and is surrounded by conserved acidic side chains (e.g., Asp^{22} and Glu^{23}), which are likely to contribute to the specificity of the intermolecular interactions of this domain (Figure 1B).

In another study, Zhou et al. (*29*) reported the X-ray crystal structure of rSMB in complex with PAI-1. The inferred binding interface between the SMB domain and PAI-1 was consistent with our NMR-derived solution structure (*28*) and with previous mutagenesis data (*27*, *30*−*33*) and again showed that the functional residues of the SMB domain were arranged in a contiguous patch on the surface (Figure 1B). Although the backbone fold from the X-ray structure was quite consistent with our NMR structure, the disulfide bond arrangements derived from the two studies differed. These differences raised the possibility that the overall fold of the active SMB molecule may be compatible with additional arrangements of the disulfide bonds, and this hypothesis has some theoretical and experimental support (*28*). However, all of these structures (*28*, *29*) contain the disulfide bond between Cys^{25} and Cys^{31} that defines the PAI-1-binding hydrophobic surface.

The complexities of this issue have been compounded by recent NMR studies of the SMB domain isolated from plasma VN (*34*, *35*). Although the structure statistics indicate that the solution structure determination (*34*) is of extremely low quality, these authors nevertheless conclude that the disulfide bond arrangement and overall fold of the plasma VN-derived SMB domain differ significantly from that reported in the previous studies (*28*, *29*). Importantly, the Cys^{25}−Cys^{31} disulfide bond is not present, and the hydrophobic interaction face is no longer defined. An explanation for these differences was suggested by Mayasundari et al. (*34*): the bacterially expressed rSMB forms used by Kamikubo et al. (*28*) and Zhou et al. (*29*) might represent disulfide-scrambled intermediate isomers of the "native" SMB domain obtained from plasma. It is possible that the two forms of the domain, recombinant and plasma derived, do in fact have different structures and that these forms of the protein differ in PAI-1 binding activity. However, in the absence of a definitive structure for the plasma-derived SMB domain, or of any published report that it actually binds PAI-1, we cannot make a comparison here. In the current report, we provide evidence that the biologically active recombinant form of SMB employed in our studies is correctly folded to the lowest energy state and that intermediate isomers are inactive. Further, we show by comparison of the NMR spectra that rSMB (residues 1−45) obtained by refolding of the reduced, denatured protein and the folded portion of rSMB (residues 1−51) obtained by affinity chromatography (*25*, *28*) are identical in structure and capable of binding the conformation-specific monoclonal antibody mAb 153 as a model for PAI-1 binding. Taken together, these results show that the stable form of the recombinant protein corresponds to the lowest thermodynamic energy state and that this state is fully active in the PAI-1-binding assay.

EXPERIMENTAL PROCEDURES

Materials. All chemicals were of the highest analytical grade commercially available. Materials were obtained as follows: cyanogen bromide (CNBr), ampicillin, kanamycin, carbenicillin, reduced glutathione (GSH), oxidized glutathione (GSSG), 4-methylumbelliferyl-*p*-guanidinobenzoate hydrochloride (MUGB), and dimethy sulfoxide (DMSO) were from Sigma (St. Louis, MO); trifluoroacetic acid (TFA) was from Pierce (Rockford, IL); high-performance liquid chromatography (HPLC) grade acetonitrile was from EM Science (Gibbstown, NJ); isotopically labeled compounds, including $^{15}NH_4Cl$, $(^{15}NH_4)_2SO_4$, and $[^{13}C_6]$glucose were from Cambridge Isotope Laboratories (Andover, MA); dithiothreitol (DTT) was from Bio-Rad Laboratories (Hercules, CA); trypsin (sequencing grade) was from Roche Diagnostics (Indianapolis, IN). High molecular weight urokinase plasminogen activator (uPA) was purchased from EMD Biosciences (La Jolla, CA), and urea-activated VN was prepared as described previously (*36*). Anti-VN mAb 153 was generated in mice immunized with urea-activated human VN as reported (*23*). This mAb recognizes and binds to the conformation-dependent epitope created by residues 22−31 of the SMB domain (*28*, *30*). A Fab fragment of mAb 153 was prepared using the ImmunoPure Fab preparation kit (Pierce). In brief, mAb 153 (7 mg) was incubated with 3.6 mL of a 50% slurry of papain-immobilized gel for 5 h at 37 °C, and then the digest was subjected to affinity chromatography using a protein A column. Under these conditions, the Fab fragment flows through the column. Further purification was achieved by applying the flow-through containing

the Fab fragment to a HiLoad Superdex 75 gel filtration column (1.6 × 60 cm; Amersham Biosciences, Piscataway, NJ) equilibrated with phosphate-buffered saline (PBS, pH 7.3). The recombinant stable active form of human PAI-1 was purified from transformed *E. coli* BL21 cells (clone 14-1b; the kind gift of Dr. Daniel A. Lawrence) by heparin affinity chromatography, followed by gel filtration using a HiLoad Superdex 75 column equilibrated with 5 mM phosphate buffer containing 0.345 M NaCl (pH 6.5). The specific inhibitory activity of PAI-1 was measured by titration against uPA in a single-step chromogenic assay using the uPA substrate S-2444 (Chromogenix; DiaPharma Inc., West Chester, OH). The specific activity of uPA was determined by active site titration with the fluorogenic substrate MUGB as previously described (*37*). The concentration of active PAI-1 was calculated from the uPA inhibition curves assuming a 1:1 stoichiometry between PAI-1 and uPA.

Preparation of the Active Form of rVN1−51. To prepare the active form of the SMB domain (amino acid residues 1−51, VN1−51; see Figure 1A), a fusion protein containing the NH_2-terminal 97 amino acid residues of VN (VN1−97) linked to the COOH terminus of thioredoxin was expressed in transformed *E. coli* BL21*trxB*(DE3) as previously described (*25*, *28*). Expression of rVN197 was induced by incubating the cells with 0.5 mM isopropyl β-D-thiogalactopyranoside (IPTG) at room temperature for 2.5 h. To prepare ^{15}N- and ^{13}C-labeled rVN1−97, the transformed cells were cultured at 37 °C in M9 minimal medium that was supplemented with 0.1% $^{15}NH_4Cl$, 0.1% $(^{15}NH_4)_2SO_4$, and 0.1%[$^{13}C_6$]glucose. The expression of $^{15}N/^{13}C$-labeled rVN1−97 was induced by incubating the bacteria with IPTG as described above. In all cases, the isolated rVN1−97 was cleaved with CNBr, and the resulting active form of VN (1−51) was purified by immunoaffinity chromatography using an anti-SMB mAb 153-conjugated Cellufine column (1.0 × 6 cm) as previously described (*25*, *28*). Only the active form of rVN1−51 bound to the column, and it was eluted with 0.1% (v/v) aqueous TFA. For further purification, the eluted rVN1−51 was subjected to reversed-phase (RP) HPLC using a preparative BetaBasic CN column (21.2 × 150 mm; Western Analytical Products). The active form of rVN1−51 was eluted with a linear gradient (from 0% to 55%) of 80% acetonitrile in 0.1% (v/v) aqueous TFA at a flow rate of 6 mL/min. RP-HPLC was carried out on an AKTApurifier system (Amersham Biosciences) at 4 °C. Finally, the purified peptides were lyophilized, and the resulting powders were dissolved in 20 mM sodium phosphate buffer (pH 7.5) and stored at −80 °C until NMR analysis and/or oxidative folding studies. Protein concentration was determined by amino acid composition analysis. The average mass of rVN1−51 was determined by matrix-assisted laser desorption/ionization time-of-flight (MALDI-TOF) mass spectrometry (Mass Spectrometry Core Facility, The Scripps Research Institute, La Jolla, CA).

Oxidative Folding of the Reduced and Denatured SMB Domain. In the present study, we performed in vitro oxidative folding experiments using reduced and denatured rVN1−45 instead of rVN1−51. We took this approach because it was expected that the folding intermediates from rVN1−45 would be more easily resolved by RP-HPLC than those from rVN1−51 since the latter peptide contains COOH-terminal homoserine lactone that can be converted to a COOH-terminal homoserine (*28*). Moreover, the original NMR spectra of rVN1−51 indicated that the COOH-terminal 10 residues (residues 42−51) were disordered in solution (*28*). This approach was further justified since active rVN1−45 had the same PAI-1 and mAb 153 binding activities as those of rVN1−51 (see Figure 3). The active form of rVN1−45 was prepared by trypsin digestion of active rVN1−51 at a ratio of 50:1 substrate to enzyme (w/w) (see Figure 1A). Trypsin digestion was performed in 20 mM sodium phosphate buffer (pH 7.5) at 37 °C for 17 h. After trypsin digestion, the active form of rVN1−45 was purified by RP-HPLC using a preparative BetaBasic CN column as described in the preceding paragraph. To prepare the fully reduced and denatured SMB domain, active rVN1−45 (350 μg/mL) was incubated in 25 mM Tris-HCl buffer, pH 8.5, containing 1 mM EDTA, 6 M guanidine hydrochloride, and 10 mM DTT. The reaction was carried out at 45 °C for 1 h. The reduced and denatured form of rVN1−45 was purified by RP-HPLC using a preparative BetaBasic CN column and then lyophilized. To carry out control oxidative folding experiments in the absence of redox agent, we added 520 μL of 50 mM Tris-HCl buffer (TB/EDTA, pH 8.5) containing 1 mM EDTA to the reduced and denatured rVN1−45 powder (40 μg), and the solution was incubated for up to 48 h at room temperature. To monitor oxidative folding in the presence of redox agents, we dissolved the powder containing the reduced and denatured rVN1−45 (40 μg) into 520 μL of TB/EDTA at either pH 8.5 or pH 7.5. Oxidative folding was subsequently initiated by incubating the reduced and denatured rVN1−45 solution with either 1 mM GSH, 0.2 mM GSSG, or a mixture of 1 mM GSH and 0.2 mM GSSG at room temperature. Oxidative folding intermediates were trapped at selected times by acid quenching using 0.5% (v/v) aqueous TFA. After acid quenching, the folding intermediates and refolded rVN1−45 were analyzed and purified by RP-HPLC using a semipreparative BetaBasic CN column (4.6 × 250 mm; Western Analytical Products) with a linear gradient (from 0% to 55%) of 80% acetonitrile in 0.1% (v/v) aqueous TFA at a flow rate of 0.5 mL/min. To check the purity of the refolded rVN1−45, we performed analytical RP-HPLC using a Vydac C18 column (4.6 × 250 mm; Western Analytical Products) or a Vydac C8 column (4.6 × 250 mm; Western Analytical Products) with a linear gradient (from 22% to 30%) of 80% acetonitrile in 0.1% (v/v) aqueous TFA at a flow rate of 0.5 mL/min. The refolded form of $^{15}N/^{13}C$-labeled rVN1−45 was also prepared by oxidative folding of the reduced form with TB/EDTA (pH 8.5) containing 1 mM GSH and 0.2 mM GSSG for 24 h. After lyophilization of stably refolded rVN1−45 and its various folding intermediates, the resulting powders were reconstituted with water or 20 mM sodium phosphate buffer (pH7.5) and then stored at −80 °C. The molecular masses of active rVN1−45, reduced rVN1−45, stably refolded rVN1−45, or the various folding intermediates were determined by electrospray ionization (ESI) mass spectrometry using a PE SCIEX API III electrospray mass spectrometer (Perkin-Elmer, Applied Biosystems, Foster City, CA). The protein concentrations of rVN1−45 and reduced rVN1−45 were determined by measuring absorbance at 280 nm using an extinction coefficient of 0.836 and 0.743 mL mg^{-1} cm^{-1}, respectively. These extinction coefficient values were determined by using

the software program ProtParam (http://au.expasy.org/tools/protparam.html).

Preparation of Complexes between Stably Refolded rVN1−45 and mAb 153. To prepare refolded rVN1−45 in complex with the Fab fragment of mAb 153, the refolded form of $^{15}N/^{13}C$-labeled rVN1−45 (75 μM) was incubated with the Fab (140 μM) in 300 μL of PBS (pH 7.3) for 1 h at room temperature at a molar ratio of approximately 1:2. The mixture was subsequently subjected to analysis by NMR spectroscopy.

NMR Spectroscopy. The backbone assignment (*28*) was verified using a 3D HNCA recorded on a Bruker DRX600 spectrometer equipped with a CryoProbe system (CPTXI600). The data set was collected using 2048* (t_1) × 64* (t_2) × 40* (t_3) data points with a spectral width of 9615.385 Hz (^{1}H), 3621.876 Hz (^{13}C), and 1824.418 Hz (^{15}N) and the carrier at 4.79, 57.76, and 120.2 ppm, respectively. The ^{15}N−^{1}H HSQC spectrum of free rVN1−45 was acquired on a Bruker Avance500 spectrometer with standard pulse sequences and was collected with a spectral width of 8012.82 Hz and 2048* data points in the ^{1}H dimension and 1666.67 Hz and 64 data points in the ^{15}N dimension. The ^{15}N−^{1}H HSQC spectrum of the rVN1−45/Fab complex was acquired on a Bruker Avance900 spectrometer with a spectral width of 14367.81 Hz and 2048 data points in the ^{1}H dimension and 2735.79 Hz and 64 data points in the ^{15}N dimension. All spectra were acquired at 293 K. The NMR spectra were processed using NMRPipe (*38*) and analyzed using NMRView (*39*).

Binding Studies. Binding of rSMB domains (i.e., active rVN1−51, active rVN1−45, refolded rVN1−45, or folding intermediates) to PAI-1 or mAb 153 was determined by competitive surface plasmon resonance (SPR) analysis using the BIAcore TM3000 biosensor system and reagents (amine-coupling kit and CM5 sensor chips) from BIAcoreAB (Uppsala, Sweden) as previously described (*28*). In brief, the PAI-1 samples (25 nM) were preincubated with the various rSMB domains (25 nM) at room temperature for 10 min and then passed over sensor chips coated with urea-activated VN at a flow rate of 20 μL/min. SPR analysis was performed in BIAcore certified HBS-EP buffer (10 mM HEPES, pH 7.4, containing 0.15 M NaCl, 3 mM EDTA, and 0.005% surfactant P20). The amount of bound PAI-1 on the sensor chip was determined by measuring the resulting signal expressed as resonance units. All experiments were performed at 25 °C. The sensor chip was regenerated by washing with 0.1 M HCl. The binding affinity of rSMB for mAb 153 was also determined by competitive BIAcore experiments using urea-activated VN-immobilized sensor chips. Briefly, 25 nM rSMB was incubated with 25 nM mAb 153 Fab fragment at room temperature for 60 min, and then the mixture was injected onto the chip. A control experiment demonstrated that the Fab fragment of mAb 153 bound to urea-activated VN on the sensor chip with a K_D value of 19 nM.

RESULTS

Oxidative Folding of rVN1−45 in the Absence of Redox Agents. Oxidative refolding experiments were initially performed in Tris-HCl buffer (pH 8.5) in the absence of redox agents. The folding intermediates formed after incubation for various times were trapped at various times by acidification with 0.5% (v/v) aqueous TFA and then analyzed by reversed-phase (RP) HPLC. As shown in Figure 2A, the fully reduced form of rVN1−45 containing eight free cysteines (mass of 5168 Da) disappeared by 4 h after initiation of the folding reaction, and a number of intermediate isomers appeared. A total of 14 fractions (peaks 1−14) consisting of partially oxidized and scrambled intermediates were identified by RP-HPLC, and each was then analyzed by ESI mass spectrometry (Table 1). For example, analysis of the peaks formed after 1 h (i.e., peaks 1−4) demonstrated that these intermediates were partially oxidized rVN1−45 isomers and that peaks 1, 2, and 3 represented rVN1−45 with two intact disulfide bonds and a molecular mass of 5164. Peak 4 was rVN1−45 with one disulfide bond and a mass of 5166 Da. The folding intermediates formed after incubaiton for 16, 24, or 48 h continued to show a high degree of heterogeneity. Ten fractions, representing the material in peaks 5−14 from the 48 h sample (Figure 2A), contained fully oxidized, four-disulfide intermediate isomers with a mass of 5160 Da (Table 1). The refolding reaction did not reach completion even after 48 h incubation in Tris-HCl buffer alone (i.e., without redox agent).

Effect of Glutathione Redox Buffers on Oxidative Folding. It is well-known that redox agents such as glutathione, mercaptoethanol, and cysteine significantly accelerate the rate of oxidative folding of reduced peptides and proteins (*40*−*44*). To investigate the effect of redox agents on the oxidative folding of the reduced and denatured rVN1−45, we carried out the folding reaction in Tris-HCl buffer (pH 8.5) containing 1 mM reduced glutathione (GSH) and 0.2 mM oxidized glutathione (GSSG). Under these conditions, the completely reduced form of rVN1−45 and the partially oxidized forms of rVN1−45 detected in peaks 1, 2, 3, and 4 disappeared within 60 min, and this disappearance was associated with the appearance of the fully oxidized four-disulfide intermediate isomers in peaks 5, 6, 7, 8, 9, and 14 (Figure 2B). After 5 and 24 h, the intermediate isomers detected in peaks 5, 6, 7, 8, and 9 had completely disappeared, and a new rVN1−45 isomer with a stable conformation had accumulated in peak 14. Thus, peak 14 seems to be a stable refolded form of fully oxidized VN1−45, while the isomers detected in peaks 5, 6, 7, 8, and 9 are four-disulfide intermediates that appear to be scrambled (see also Table 1). Quantitative analysis showed that the amount of the stably refolded form increased linearly, reaching 80% of the total by 5 h and >95% after 24 h (Figure 2D). In contrast, the amount of this form remained at less than 5% of the total in the absence of redox buffer even after 48 h. High recovery (>90%) of the refolded rVN1−45 was also observed when oxidized folding was performed in the presence of either 1 mM GSH or 0.2 mM GSSG (data not shown). To check the purity of the refolded rVN1−45, we performed analytical RP-HPLC using a C18 or C8 column. As shown in the inset of Figure 2B, the stably refolded form of rVN1−45 had high (>95%) purity.

The rate of oxidative folding is greater at alkaline pH compared to neutral pH, primarily because of the pH dependence of disulfide exchange reactions involving cysteine thiols with a pK_a value of approximately 9 (*45*). To examine the effect of pH on the rate of oxidative folding of reduced rVN1−45, we repeated the folding experiment but

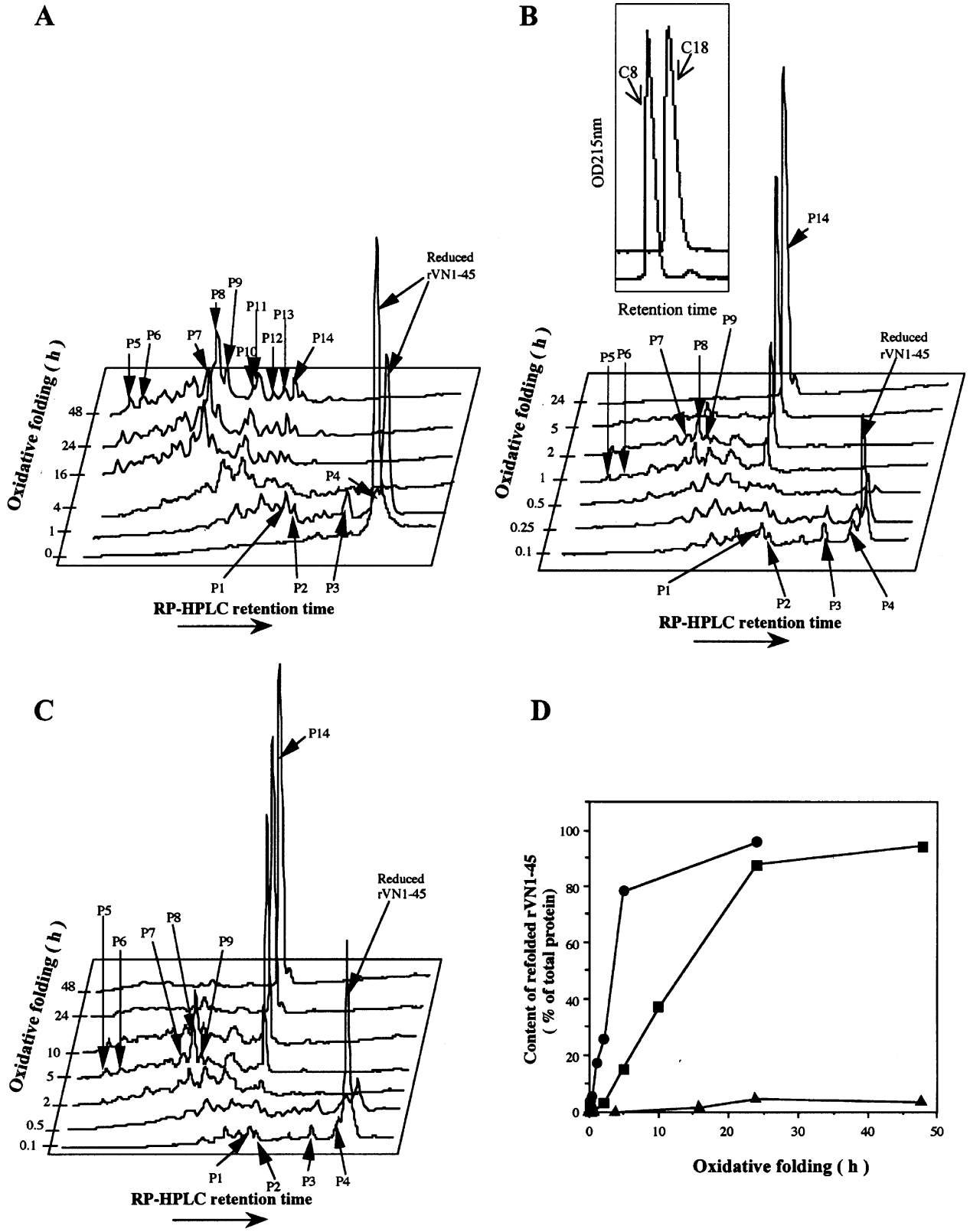

FIGURE 2: Analysis of the refolding of reduced and denatured rVN1−45. Panels A−C: Reversed-phase HPLC analysis. The solid lines in each panel show the absorbance of the eluate at 215 nm. (A) Folding performed in the presence of Tris-HCl buffer containing only 1 mM EDTA (TB/EDTA) (pH 8.5). (B) Folding performed in TB/EDTA buffer (pH 8.5) containing 1 mM GSH and 0.2 mM GSSG. Inset: Analytical RP-HPLC analysis of refolded rVN1−45 using either Vydac C18 or C8 columns with a linear gradient (from 22% to 30%) of 80% acetonitrile in 0.1% (v/v) aqueous TFA at a flow rate of 0.5 mL/min. The chromatograms show that the stably refolded form of rVN1−45 has high (>95%) purity. (C) Folding performed in the TB/EDTA buffer (pH 7.5) containing 1 mM GSH and 0.2 mM GSSG. (D) Determination of the relative amount of stably refolded rVN1−45 in the above preparations. In each case, the amount of stably refolded rVN1−45 was determined by integration of peak 14 and was expressed as the percentage of the total rVN1−45 used in the refolding experiment. Closed triangles, folding performed in TB/EDTA (pH 8.5) alone; closed circles, folding performed in TB/EDTA buffer (pH 8.5) containing 1 mM GSH and 0.2 mM GSSG; closed squares, folding performed in TB/EDTA buffer (pH 7.5) containing 1 mM GSH and 0.2 mM GSSG.

Table 1: Refolded rVN1−45 and Folding Intermediates Produced by Oxidative Folding

peak	mass (Da) obsd[a]	mass (Da) calcd	rVN1−45 form
P1	5164	5160	2 disulfide rVN1−45
P2	5164	5160	2 disulfide rVN1−45
P3	5164	5160	2 disulfide rVN1−45
P4	5166	5160	1 disulfide rVN1−45
P5	5159	5160	fully oxidized rVN1−45
P6	5159	5160	fully oxidized rVN1−45
P7	5160	5160	fully oxidized rVN1−45
P8	5160	5160	fully oxidized rVN1−45
P9	5160	5160	fully oxidized rVN1−45
P10	5159	5160	fully oxidized rVN1−45
P11	5159	5160	fully oxidized rVN1−45
P12	5159	5160	fully oxidized rVN1−45
P13	5160	5160	fully oxidized rVN1−45
P14	5160	5160	refolded VN1−45
active rVN1−45	5160	5160	
reduced rVN1−45	5167	5168	

[a] Molecular mass of rVN1−45 was determined by ESI mass spectrometry.

at pH 7.5 instead of pH 8.5. As shown in Figure 2C, oxidative folding of reduced rVN1−45 again proceeded via partially oxidized and scrambled four-disulfide intermediates, and the stably refolded form of rVN1−45 again accumulated in peak 14. Quantitative analysis (Figure 2D) showed that, at pH 7.4, the amount of stably refolded rVN1−45 increased to approximately 80% of the total after 24 h and to approximately 90% after 48 h. Thus, the refolding reaction at pH 7.5 was slower than the reaction at pH 8.5. More specifically, the time to accumulate 50% of the stably refolded rVN1−45 at pH 7.5 was about 4 times longer than that at pH 8.5 (14 vs 3 h).

Binding of Stably Refolded rVN1−45 to PAI-1 and mAb 153. To evaluate the biological activity of the refolded rVN1−45 peptides, we determined their ability to bind to PAI-1 and to a conformation-dependent mAb using competitive BIAcore analysis on VN-immobilized sensor chips. As shown in Figure 3A, when the nonreduced active form (25 nM) of either rVN1−51 or rVN1−45 was incubated with 25 nM PAI-1, they both significantly inhibited the binding of PAI-1 to the VN-coated sensor chips. Importantly, the stably refolded form of rVN1−45 (i.e., peak 14, Figure 2B) also competitively inhibited PAI-1 binding, and it had the same specific inhibitory activity as that of active rVN1−51 used in our original experiments (*28*). In contrast, neither the fully reduced and denatured form of rVN1−45 nor any of the scrambled four-disulfide intermediates inhibited PAI-1 binding. Figure 3B shows that the stably refolded rVN1−45 also binds to a Fab fragment of mAb 153 and that the folding intermediates do not. This mAb recognizes the conformation-dependent epitope created by residues 22−31 in the SMB domain which is close to the binding site in the SMB domain for PAI-1 (*28*, *30*). Thus, of the species generated during the refolding reaction, only the stably refolded rVN1−45 significantly inhibited the binding of the mAb to the VN-coated sensor chips. The disulfide-scrambled intermediates had no effect on this interaction. Importantly, the inhibitory activity of the stably refolded peptide was the same as that of the active rSMB peptides originally isolated from the transformed bacteria and not subjected to the refolding (i.e., rVN1−45 and rVN1−51) (*25*, *28*).

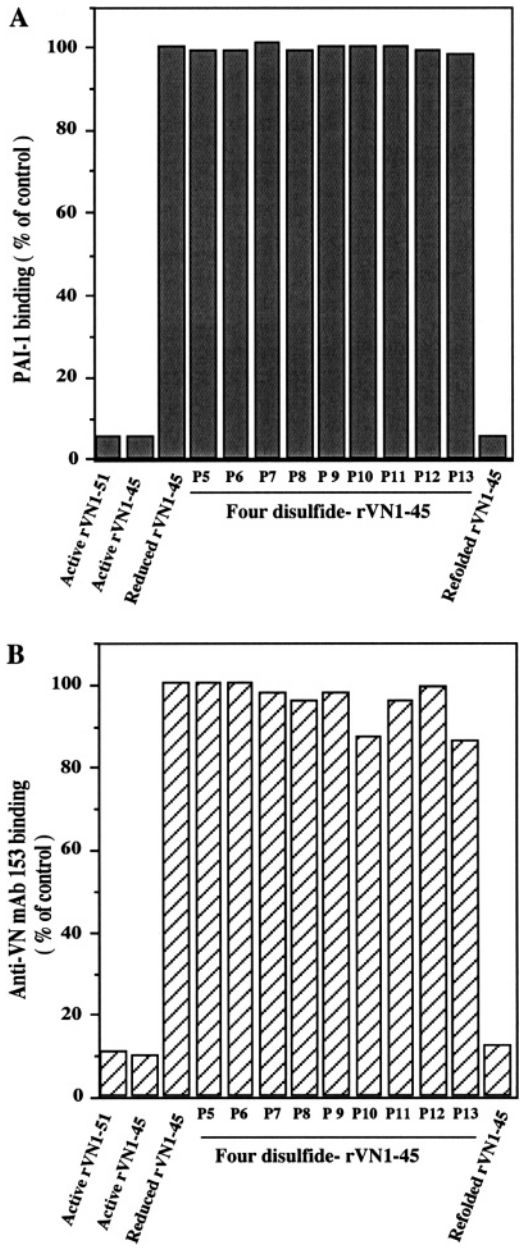

FIGURE 3: Binding of refolded rVN1−45 and its folding intermediates to PAI-1 (A) and to mAb 153 (B) as determined by competitive surface plasmon resonance analysis (BIAcore). In these experiments, PAI-1 or mAb 153 samples (25 nM) were incubated with 25 nM stably refolded rVN1−45 (i.e., peak 14) or its various folding intermediates (i.e., peaks 5−13) at room temperature for 10 min (PAI-1) or 60 min (mAb 153), and then the mixtures were injected onto urea-activated VN-immobilized sensor chips. The amount of PAI-1 or mAb 153 bound to the sensor chip was determined by measuring the resulting signal expressed as resonance units. The results are compared to the binding of the original active forms of rVN1−51 and rVN1−45 (i.e., purified by binding to mAb153 columns and active without refolding) and completely reduced rVN1−45. The results are expressed as the percentage of PAI-1 (A) or mAb153 (B) that bound to the chips in the absence of competitors.

NMR Spectrum of the Stably Refolded rVN1−45. For NMR analysis, we prepared the stably refolded form of ^{15}N/^{13}C-labeled rVN1−45 by oxidative folding of the completely reduced and denatured form by incubation for 24 h using glutathione redox buffer (pH 8.5) containing 1 mM GSH and 0.2 mM GSSG. The peptide was purified by RP-HPLC and shown to bind to both PAI-1 and mAb 153 (data not

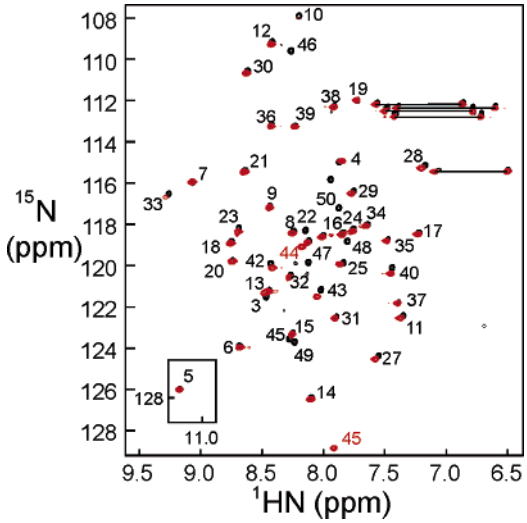

FIGURE 4: HSQC spectra of rSMB. Overlay of the ^{1}H−^{15}N HSQC spectrum of the stably refolded form of ^{15}N/^{13}C-labeled rVN1−45 (red) with that of the original active ^{15}N-labeled rVN1−51 (*28*) (black). Where ^{1}H−^{15}N cross-peaks of the backbone amides in rVN1−45 differ from those in rVN1−51, they are labeled in red.

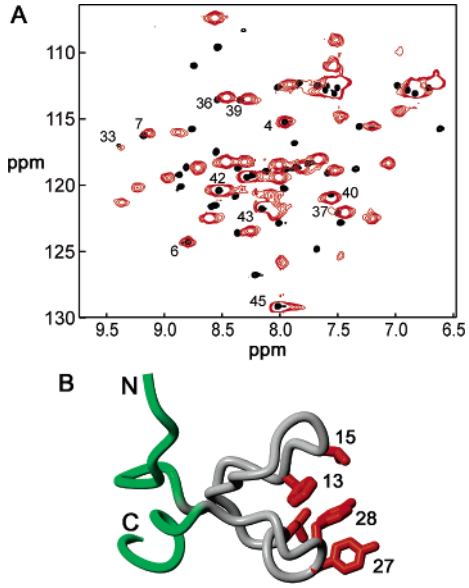

FIGURE 5: NMR analysis of complexes between stably refolded rVN1−45 and mAb 153. (A) Superposition of the ^{1}H−^{15}N HSQC spectrum (red) from the refolded form of ^{15}N/^{13}C-labeled rVN1−45 in complex with anti-VN mAb 153 onto that of the free refolded rVN1−45 (black). Cross-peaks that are unchanged in position between the two spectra are labeled. The cross-peak of Cys 5 (see Figure 4) has been omitted for clarity. (B) Positions of the residues with unchanged cross-peaks in part A mapped onto the structure of rSMB (*28*). Hydrophobic side chains in rSMB are shown in red. Green: residues with unchanged cross-peaks. Gray: residues with shifted cross-peaks. Structure prepared in MOLMOL (*49*).

shown). NMR data were obtained by using approximately 80 μM refolded peptide. The ^{1}H−^{15}N HSQC spectrum obtained with this material is shown in Figure 4, overlaid with the spectrum of the active rVN1−51 employed in our previous studies (*28*). It is clear that the refolded rVN1−45 has the same structure as the active rVN1−51 that was employed in our original studies and was not subjected to the reduction and unfolding process.

NMR Spectrum of Stably Refolded rVN1−45 in Complex with mAb 153. To verify that the refolded rSMB has the 3-D structure required for binding to the conformation-specific antibody, and by inference to PAI-1, we performed NMR analysis of refolded rSMB in complex with mAb 153. PAI-1 itself cannot be used under these conditions, as it is unstable and difficult to keep in solution at high concentrations (>140 μM) for long periods (*5*−*8*). The binding epitope in the SMB domain for the mAb is very close to that for PAI-1 since the mAb specifically inhibits PAI-1 binding to urea-activated VN (*23*, *24*). Moreover, this mAb recognizes the same conformation-dependent epitope created by residues 22−31 of the SMB domain, including Leu^{24}, Tyr^{27}, and Tyr^{28} (*28*, *30*). Complexes between the stably refolded form of ^{15}N/^{13}C-labeled rVN1−45 and mAb 153 were prepared by incubating the refolded form with the mAb at a molar ratio of approximately 1:2. The ^{15}N−^{1}H HSQC spectrum of the ^{15}N-labeled rSMB bound to the mAb is shown in Figure 5A, overlaid with the spectrum of the free rSMB. The antibody-bound rSMB shows cross-peaks that are greatly broadened, consistent with binding to the ∼50 kDa Fab fragment of mAb153. Some of the cross-peaks are significantly shifted in the complex, compared with their positions in free rSMB, while others appear to be largely unchanged. This behavior is consistent with binding of the mAb to a specific site on rSMB, which is mapped onto one of the published NMR structures (*28*) in Figure 5B.

DISCUSSION

In the past four years, considerable information has been generated about the structure of the SMB domain and the PAI-1 binding site within it. Biochemical experiments (*25*) strongly implicated a linear, uncrossed disulfide pattern for the recombinant SMB domain. However, the X-ray crystal structure of the SMB domain in complex with PAI-1 (*29*) showed a different disulfide bonding pattern, which nevertheless retained the Cys^{25}−Cys^{31} disulfide bond that defined the PAI-1 binding surface. Surprisingly, these authors did not attempt to reconcile the difference in their structure with the previously reported disulfide pattern. In fact, no reference was made in this paper to the results of Kamikubo et al. (*25*). The proteins were prepared in a very similar way, by expression in *E. coli* of a protein fusion (GST for the X-ray structure and thioredoxin for the biochemical experiments), followed by CNBr cleavage. Both were purified by HPLC, but in the case of the biochemical experiments (*25*), the protein was also purified on an affinity column containing the conformation-specific antibody mAb 153, ensuring that only the rSMB molecules with PAI-1 binding activity were present in the subsequent experiments. No such purification step is described in the X-ray paper, which describes characterization of the final protein by mass spectrometry: the mass was consistent with the presence of four disulfide bonds, but in the absence of the description of a purification protocol involving affinity with biological partners, it is possible that there could be a mixture of species, each with four disulfide bonds, but in different patterns. If this were the case, it is possible that the crystallization process may have selected one of the isomers preferentially, perhaps an isomer that was not the same active form that was prepared and characterized in the biochemical experiments of Kamikubo et al. (*25*).

Table 2: Biochemical Properties of SMB Variants

SMB domain	PAI-1 binding K_D[a]	disulfide bond arrangement	ref
rSMB Trx fusion in *E. coli*	0.34×10^{-9}	C5−C9, C19−C21 C25−C31, C32−C39	this work, *24*, *25*, *28*
rSMB GST fusion in *E. coli*	1×10^{-9}	C5−C21, C9−C39 C25−C31, C19−C32	*29*
SMB from plasma VN	not reported	C5−C9, C19−C31 C21−C32, C25−C39	*34*, *35*

[a] Dissociation constant.

In the meantime, we had undertaken an NMR solution study of the recombinant SMB domain. Structures were determined by employing ^{15}N-labeled protein and assuming the disulfide bonding pattern established in the biochemical experiments. The NMR data were perfectly consistent with the linear, uncrossed disulfide bonding pattern of Kamikubo et al. (*25*). After publication of the X-ray structure, we repeated the structure determination of the SMB domain employing both the disulfide pattern used in the X-ray study and another disulfide pattern unrelated to either of these. All of the disulfide bonding patterns were completely consistent with the NMR data, and there was very little energy difference between these patterns in the final solution structures. The structures incorporating all three disulfide bonding patterns were completely superimposable with the structure of the SMB domain in the X-ray structure of the PAI-1 complex. We concluded that all of these disulfide bonding patterns were potentially present in the SMB domain in solution and that alternative disulfide bond arrangements could exist in the tightly packed core of the domain as long as the critical Cys^{25}−Cys^{31} disulfide bond is preserved (*28*).

At the same time, a third group was performing an NMR solution structure determination on the SMB domain derived by proteolysis of plasma vitronectin (*34*). Proteins derived from plasma cannot be labeled with stable isotopes for NMR, so the structure determination was performed using proton data only. This structure not only was different in disulfide pattern but showed a completely different global fold compared to the recombinant form as determined either by X-ray crystallography (*29*) or by NMR (*28*). The quality of the structure of the plasma-derived SMB domain is not good, and we believe it may be incorrect. Importantly, the authors nowhere demonstrate or state that the molecule prepared from plasma vitronectin is active in the PAI-1 assay. Since this is at present the only assay for biological activity of the SMB domain, the biological relevance of plasma-derived SMB is unclear. Instead of discussing this potential problem, these authors imply that the recombinant material used in the NMR and X-ray experiments may be incorrectly folded. The differences between the published structures are summarized in Table 2.

The above circumstances form the background for the present paper. We show first that the recombinant form of SMB that was used for our NMR structure determination (*28*) constitutes the thermodynamically lowest energy form. Further, it is active in PAI-1 binding. The intermediates that are formed during the refolding reaction, presumably with incorrect disulfides, have been isolated and characterized. They are inactive in the PAI-1 binding assay but are converted over time to the active form. These results contradict the assertion by Mayasundari et al. (*34*) that the recombinant SMB is an incorrectly disulfide-bridged, nonnative form.

To put these apparently confusing results into context, it is necessary to consider possible changes that may occur in the SMB domain in vivo. Vitronectin is a very labile protein and can undergo dramatic conformational changes and even disulfide exchange upon incubation or during its purification (*46*). Importantly, VN is known to undergo a conformational change that potentiates PAI-1 binding (*47*). Thus, the biological activity of VN and SMB must be monitored as the protein is purified and characterized. The only biological assays currently available for correctly folded SMB are its ability to bind to PAI-1, to the urokinase receptor, and to conformation-dependent mAbs. These assays specifically test for the presence of an intact PAI-1 binding site, which may be cryptic or even in an inactive conformation in the plasma protein that circulates in the absence of PAI-1. Since no information on the biological activity of the plasma VN-derived SMB was provided in the report by Mayasundari et al. (*34*), we cannot evaluate whether the starting material that was used to derive this structure was folded to give another active conformation for SMB. Thus, it is possible that the two very different backbone folds merely represent different forms of the SMB domain, one that is active in PAI-1, urokinase receptor, and mAb binding and one that is inactive.

In the work reported in this paper, we specifically address the suggestion (*34*) that the recombinant SMB domain used to obtain the NMR (*28*) and X-ray crystal structures (*29*) consisted of intermediate states with incorrect disulfide bonding patterns. Studies of the folding pathways of disulfide-bonded proteins were among the earliest in the field (*48*) and provided the main impetus for the ideas that the folding of proteins is encoded in the amino acid sequence and that the final folded state of a protein represents the thermodynamically most stable state. As long as the proper conditions are available (e.g., the presence of redox-active agents in the case of disulfides or chaperone molecules in the case of other forms of protein misfolding), kinetically trapped, misfolded intermediate forms can be resolved and allowed to progress to the normal thermodynamic minimum. The refolding pathways of a number of cysteine-rich proteins have been studied by the technique of oxidative folding (*40*−*44*). Trapping of intermediates by acid quenching allows for the structural characterization of both trapped intermediates and stably refolded proteins. The same principles have been used for the experiments described herein.

The reduced and denatured forms of the rSMB domain were prepared and then allowed to slowly refold in the presence or absence of redox reagents. The intermediates and stably refolded peptides were then purified by reversed-phase HPLC and characterized biochemically. As shown in Figure 2, in the presence of glutathione redox buffers, the completely reduced and denatured rSMB domain rapidly refolded into a single stable structure which was biologically active since it bound to PAI-1 and mAb 153 (Figure 3). None of the folding intermediates bound to PAI-1 or the mAb. The refolded rSMB was highly homogeneous according to RP-HPLC analysis (Figure 2B, inset), and the NMR spectrum of the refolded rSMB demonstrated that the backbone fold was identical to that of the active rSMB used in our original experiments (i.e., purified directly from transformed *E. coli*

and not subjected to reduction and refolding) (Figure 4). NMR experiments also showed that the refolded rSMB forms a complex with mAb 153, an indication that the refolded molecule regained the 3-D structure essential for PAI-1 binding. These results confirm that the recombinant SMB that was used to obtain the original NMR solution structure (*28*) has the lowest energy conformation in solution and that it is fully active in the PAI-1 and mAb assays.

The demonstration by NMR spectroscopy that rSMB binds to form a well-defined complex with the conformation-specific monoclonal antibody (Figure 5A) provides an important clue to the structure of the bound rSMB in the PAI-1 complex. We were unable to demonstrate the binding of PAI-1 itself to rSMB under the present conditions, due to the extreme instability of PAI-1 in solution at concentrations suitable for detection by NMR. However, it is clear from a number of studies that mAb 153 can be used as a model for the binding of PAI-1. There are several important features that should be noted in the overlaid spectra of Figure 5. For example, the two spectra are quite similar. In fact, a number of the cross-peaks (labeled in Figure 5A) are identical in the free and bound forms of rSMB, and while other cross-peaks are shifted, the overall pattern of the spectrum remains similar, indicating that there is no drastic structural change in rSMB as a result of binding. It is also noticeable that the cross-peaks in the spectrum of the bound rSMB (red) are much broader than those of the free protein (black). This is a strong indication that tight binding has occurred and, thus, that the rSMB is now tumbling in solution with a correlation time that is comparable to that of the mAb (molecular mass 50 kDa). In addition, it appears from the pattern of shifted cross-peaks that the mAb binds to a specific site on rSMB: while we have not yet made resonance assignments for rSMB in the complex, the locations of the residues corresponding to the unchanged cross-peaks in the NMR spectrum can be mapped onto the 3-D structure, giving a picture of the areas that are not affected by binding and leaving areas that are candidates for the location of the binding site. Such a map is shown in Figure 5B. The green areas show the backbone location of the unchanged cross-peaks in Figure 5A. The side chains of all of the hydrophobic amino acids in the molecule are shown: it appears that mAb 153 makes contact with the same hydrophobic face that has been implicated in binding of PAI-1 and identified in both the X-ray (*29*) and NMR (*28*) structure determinations.

CONCLUSIONS

According to our redox-mediated folding experiments, the recombinant form of the SMB domain of vitronectin is not a folding intermediate but rather takes up a highly stable conformation that corresponds exactly to the previously published solution structure. This form of rSMB is also fully active in the PAI-1 and mAb 153 binding assays, and we have been able to map the binding surface of the mAb (and, by implication, of PAI-1) to the face of the SMB domain that contains a group of conserved hydrophobic side chains that have been previously implicated in PAI-1 binding in mutagenesis experiments. We speculate that the plasma-derived form of the SMB domain may have a different backbone fold from rSMB, perhaps corresponding to a structure that is inactive in binding to PAI-1. The structures of the various functional forms of the SMB domain of vitronectin, and the means of their interconversion in vivo, remain to be determined. Further work is needed to explicitly define the structural differences between the plasma-derived SMB and the recombinant form. As well, the relationship between these forms and the native form(s) present in the intact VN remains to be delineated.

ACKNOWLEDGMENT

We acknowledge the technical assistance of Nancy V. Wagner. We thank Dr. Michael J. Churchill (The Scripps Research Institute) for much help with ESI mass spectrometry analysis and Dr. Jui-Yoa Chang (The University of Texas) for helpful discussions.

REFERENCES

1. Tomasini, B. R., and Mosher, D. F. (1991) Vitronectin, *Prog. Hemostasis Thromb. 10*, 269−305.
2. Preissner, K. T., and Seiffert, D. (1998) Role of vitronectin and its receptors in haemostasis and vascular remodeling, *Thromb. Res. 89*, 1−21.
3. Schvartz, I., Seger, D., and Shaltiel, S. (1999) Vitronectin, *Int. J. Biochem. Cell Biol. 31*, 539−544.
4. Dellas, C., and Loskutoff, D. J. (2005) Historical analysis of PAI-1 from its discovery to its potential role in cell motility and disease, *Thromb. Haemostasis 93*, 631−640.
5. Hekman, C. M., and Loskutoff, D. J. (1985) Endothelial cells produce a latent inhibitor of plasminogen activators that can be activated by denaturants, *J. Biol. Chem. 260*, 11581−11587.
6. Mottonen, J., Strand, A., Symersky, J., Sweet, R. M., Danley, D. E., Geoghegan, K. F., Gerard, R. D., and Goldsmith, E. J. (1992) Structural basis of latency in plasminogen activator inhibitor-1, *Nature 355*, 270−273.
7. Shore, J. D., Day, D. E., Francis-Chmura, A. M., Verhamme, I., Kvassman, J., Lawrence, D. A., and Ginsburg, D. (1995) A fluorescent probe study of plasminogen activator inhibitor-1. Evidence for reactive center loop insertion and its role in the inhibitory mechanism, *J. Biol. Chem. 270*, 5395−5398.
8. Wind, T., Hansen, M., Jensen, J. K., and Andreasen, P. A. (2002) The molecular basis for anti-proteolytic and non-proteolytic functions of plasminogen activator inhibitor type-1: roles of the reactive centre loop, the shutter region, the flexible joint region and the small serpin fragment, *Biol. Chem. 383*, 21−36.
9. Declerck, P. J., De Mol, M., Alessi, M. C., Baudner, S., Paques, E. P., Preissner, K. T., Muller-Berghaus, G., and Collen, D. (1988) Purification and characterization of a plasminogen activator inhibitor 1 binding protein from human plasma. Identification as a multimeric form of S protein (vitronectin), *J. Biol. Chem. 263*, 15454−15461.
10. Wiman, B., Almquist, A., Sigurdardottir, O., and Lindahl, T. (1988) Plasminogen activator inhibitor 1 (PAI) is bound to vitronectin in plasma, *FEBS Lett. 242*, 125−128.
11. Mimuro, J., and Loskutoff, D. J. (1989) Purification of a protein from bovine plasma that binds to type 1 plasminogen activator inhibitor and prevents its interaction with extracellular matrix. Evidence that the protein is vitronectin, *J. Biol. Chem. 264*, 936−939.
12. Salonen, E. M., Vaheri, A., Pollanen, J., Stephens, R., Andreasen, P., Mayer, M., Dano, K., Gailit, J., and Ruoslahti, E. (1989) Interaction of plasminogen activator inhibitor (PAI-1) with vitronectin, *J. Biol. Chem. 264*, 6339−6343.
13. Lawrence, D. A., Berkenpas, M. B., Palaniappan, S., and Ginsburg, D. (1994) Localization of vitronectin binding domain in plasminogen activator inhibitor-1, *J. Biol. Chem. 269*, 15223−15228.
14. Gibson, A., Baburaj, K., Day, D. E., Verhamme, I., Shore, J. D., and Peterson, C. B. (1997) The use of fluorescent probes to characterize conformational changes in the interaction between vitronectin and plasminogen activator inhibitor-1, *J. Biol. Chem. 272*, 5112−5121.
15. Stefansson, S., and Lawrence, D. A. (1996) The serpin PAI-1 inhibits cell migration by blocking integrin alpha V beta 3 binding to vitronectin, *Nature 383*, 441−443.

16. Kjoller, L., Kanse, S. M., Kirkegaard, T., Rodenburg, K. W., Ronne, E., Goodman, S. L., Preissner, K. T., Ossowski, L., and Andreasen, P. A. (1997) Plasminogen activator inhibitor-1 represses integrin- and vitronectin-mediated cell migration independently of its function as an inhibitor of plasminogen activation, *Exp. Cell Res. 232*, 420−429.
17. Deng, G., Curriden, S. A., Wang, S., Rosenberg, S., and Loskutoff, D. J. (1996) Is plasminogen activator inhibitor-1 the molecular switch that governs urokinase receptor-mediated cell adhesion and release?, *J. Cell Biol. 134*, 1563−1571.
18. Deng, G., Curriden, S. A., Hu, G., Czekay, R. P., and Loskutoff, D. J. (2001) Plasminogen activator inhibitor-1 regulates cell adhesion by binding to the somatomedin B domain of vitronectin, *J. Cell Physiol. 189*, 23−33.
19. Wiman, B. (1995) Plasminogen activator inhibitor 1 (PAI-1) in plasma: its role in thrombotic disease, *Thromb. Haemostasis 74*, 71−76.
20. Foekens, J. A., Peters, H. A., Look, M. P., Portengen, H., Schmitt, M., Kramer, M. D., Brunner, N., Janicke, F., Meijer-van Gelder, M. E., Henzen-Logmans, S. C., van Putten, W. L., and Klijn, J. G. (2000) The urokinase system of plasminogen activation and prognosis in 2780 breast cancer patients, *Cancer Res. 60*, 636−643.
21. Andreasen, P. A., Egelund, R., and Petersen, H. H. (2000) The plasminogen activation system in tumor growth, invasion, and metastasis, *Cell Mol. Life Sci. 57*, 25−40.
22. Seiffert, D., and Loskutoff, D. J. (1991) Evidence that type 1 plasminogen activator inhibitor binds to the somatomedin B domain of vitronectin, *J. Biol. Chem. 266*, 2824−2830.
23. Seiffert, D., Ciambrone, G., Wagner, N. V., Binder, B. R., and Loskutoff, D. J. (1994) The somatomedin B domain of vitronectin. Structural requirements for the binding and stabilization of active type 1 plasminogen activator inhibitor, *J. Biol. Chem. 269*, 2659−2666.
24. Okumura, Y., Kamikubo, Y., Curriden, S. A., Wang, J., Kiwada, T., Futaki, S., Kitagawa, K., and Loskutoff, D. J. (2002) Kinetic analysis of the interaction between vitronectin and the urokinase receptor, *J. Biol. Chem. 277*, 9395−9404.
25. Kamikubo, Y., Okumura, Y., and Loskutoff, D. J. (2002) Identification of the disulfide bonds in the recombinant somatomedin B domain of human vitronectin, *J. Biol. Chem. 277*, 27109−27119.
26. Deng, G., Royle, G., Seiffert, D., and Loskutoff, D. J. (1995) The PAI-1/vitronectin interaction: two cats in a bag?, *Thromb. Haemostasis 74*, 66−70.
27. Deng, G., Royle, G., Wang, S., Crain, K., and Loskutoff, D. J. (1996) Structural and functional analysis of the plasminogen activator inhibitor-1 binding motif in the somatomedin B domain of vitronectin, *J. Biol. Chem. 271*, 12716−12723.
28. Kamikubo, Y., De Guzman, R. N., Kroon, G., Curriden, S. A., Neels, J. G., Churchill, M. J., Dawson, P. E., Oldziej, S., Jagielska, A., Scheraga, H. A., Loskutoff, D. J., and Dyson, H. J. (2004) Disulfide bonding arrangements in active forms of the somatomedin B domain of human vitronectin, *Biochemistry 43*, 6519−6534.
29. Zhou, A., Huntington, J. A., Pannu, N. S., Carrell, R. W., and Read, R. J. (2003) How vitronectin binds PAI-1 to modulate fibrinolysis and cell migration, *Nat. Struct. Biol. 10*, 541−544.
30. Royle, G., Deng, G., Seiffert, D., and Loskutoff, D. J. (2001) A method for defining binding sites involved in protein−protein interactions: analysis of the binding of plasminogen activator inhibitor 1 to the somatomedin domain of vitronectin, *Anal. Biochem. 296*, 245−253.
31. Sui, G. C., and Wiman, B. (1998) Functional effects of single amino acid substitutions in the region of Phe113 to Asp138 in the plasminogen activator inhibitor 1 molecule, *Biochem. J. 331* (Part 2), 409−415.
32. Jensen, J. K., Wind, T., and Andreasen, P. A. (2002) The vitronectin binding area of plasminogen activator inhibitor-1, mapped by mutagenesis and protection against an inactivating organochemical ligand, *FEBS Lett. 521*, 91−94.
33. De Prada, N. A., Schroeck, F., Sinner, E. K., Muehlenweg, B., Twellmeyer, J., Sperl, S., Wilhelm, O. G., Schmitt, M., and Magdolen, V. (2002) Interaction of plasminogen activator inhibitor type-1 (PAI-1) with vitronectin, *Eur. J. Biochem. 269*, 184−192.
34. Mayasundari, A., Whittemore, N. A., Serpersu, E. H., and Peterson, C. B. (2004) The solution structure of the N-terminal domain of human vitronectin: proximal sites that regulate fibrinolysis and cell migration, *J. Biol. Chem. 279*, 29359−29366.
35. Horn, N. A., Hurst, G. B., Mayasundari, A., Whittemore, N. A., Serpersu, E. H., and Peterson, C. B. (2004) Assignment of the four disulfides in the N-terminal somatomedin B domain of native vitronectin isolated from human plasma, *J. Biol. Chem. 279*, 35867−35878.
36. Yatohgo, T., Izumi, M., Kashiwagi, H., and Hayashi, M. (1988) Novel purification of vitronectin from human plasma by heparin affinity chromatography, *Cell Struct. Funct. 13*, 281−292.
37. Geiger, M., and Binder, B. R. (1987) Tissue-type plasminogen activator and urokinase: differences in the reaction pattern with the active-site titrant 4-methylumbelliferyl-*p*-guanidinobenzoate hydrochloride, *Biochim. Biophys. Acta 912*, 34−40.
38. Delaglio, F., Grzesiek, S., Vuister, G. W., Guang, Z., Pfeifer, J., and Bax, A. (1995) NMRPipe: a multidimensional spectral processing system based on UNIX pipes, *J. Biomol. NMR 6*, 277−293.
39. Johnson, B. A., and Blevins, R. A. (1994) NMRView: A computer program for the visualization and analysis of NMR data, *J. Biomol. NMR 4*, 604−613.
40. Weissman, J. S., and Kim, P. S. (1991) Reexamination of the folding of BPTI: Predominance of native intermediates, *Science 253*, 1386−1393.
41. Salamanca, S., Li, L., Vendrell, J., Aviles, F. X., and Chang, J. Y. (2003) Major kinetic traps for the oxidative folding of leech carboxypeptidase inhibitor, *Biochemistry 42*, 6754−6761.
42. Chang, J. Y., Li, L., and Lai, P. H. (2001) A major kinetic trap for the oxidative folding of human epidermal growth factor, *J. Biol. Chem. 276*, 4845−4852.
43. Chatrenet, B., and Chang, J. Y. (1993) The disulfide folding pathway of hirudin elucidated by stop/go folding experiments, *J. Biol. Chem. 268*, 20988−20996.
44. Cemazar, M., Zahariev, S., Lopez, J. J., Carugo, O., Jones, J. A., Hore, P. J., and Pongor, S. (2003) Oxidative folding intermediates with nonnative disulfide bridges between adjacent cysteine residues, *Proc. Natl. Acad. Sci. U.S.A. 100*, 5754−5759.
45. Maskos, K., Huber-Wunderlich, M., and Glockshuber, R. (2003) DsbA and DsbC-catalyzed oxidative folding of proteins with complex disulfide bridge patterns in vitro and in vivo, *J. Mol. Biol. 325*, 495−513.
46. Tomasini, B. R., and Mosher, D. F. (1988) Conformational states of vitronectin: preferential expression of an antigenic epitope when vitronectin is covalently and noncovalently complexed with thrombin-antithrombin III or treated with urea, *Blood 72*, 903−912.
47. Seiffert, D. (1997) The glycosaminoglycan binding site governs ligand binding to the somatomedin B domain of vitronectin, *J. Biol. Chem. 272*, 9971−9978.
48. Anfinsen, C. B., Harrington, W. F., Hvidt, A., Linderstrom-Lang, K., Ottesen, M., and Schellman, J. (1955) Studies on the structural basis of ribonuclease activity, *Biochim. Biophys. Acta 17*, 141−142.
49. Koradi, R., Billeter, M., and Wüthrich, K. (1996) MOLMOL: A program for display and analysis of macromolecular structures, *J. Mol. Graphics 14*, 51−55.

BI052278F